



HAL
open science

Identification of saturated and transient transverse permeability of carbon fiber fabrics

Paul Baral, Giuseppe Pedoto, Sylvain Drapier

► **To cite this version:**

Paul Baral, Giuseppe Pedoto, Sylvain Drapier. Identification of saturated and transient transverse permeability of carbon fiber fabrics. ECCM20 - Composites Meet Sustainability, EPFL (École Polytechnique Fédérale de Lausanne); Composite Construction laboratory (CCLab); Laboratory for Processing of Advanced Composites (LPAC) - EPFL, Jun 2022, Lauzanne, Switzerland. pp.1046 à 1051, 10.5075/epfl-298799_978-2-9701614-0-0 . emse-04616880

HAL Id: emse-04616880

<https://hal-emse.ccsd.cnrs.fr/emse-04616880v1>

Submitted on 19 Jun 2024

HAL is a multi-disciplinary open access archive for the deposit and dissemination of scientific research documents, whether they are published or not. The documents may come from teaching and research institutions in France or abroad, or from public or private research centers.

L'archive ouverte pluridisciplinaire **HAL**, est destinée au dépôt et à la diffusion de documents scientifiques de niveau recherche, publiés ou non, émanant des établissements d'enseignement et de recherche français ou étrangers, des laboratoires publics ou privés.



Distributed under a Creative Commons Attribution - NonCommercial 4.0 International License

IDENTIFICATION OF SATURATED AND TRANSIENT TRANSVERSE PERMEABILITY OF CARBON FIBER FABRICS

Paul Baral^a, Giuseppe Pedoto^a, Sylvain Drapier^a

a: Mines Saint-Etienne, Univ Lyon, CNRS, UMR 5307 LGF, Centre SMS, Saint-Etienne, France – paul.baral@emse.fr

Abstract: *Saturated and unsaturated transverse permeability of quasi-unidirectional carbon fiber fabric have been measured with a new test bench equipped with micro-thermocouples. A temperature gradient is detected when the cold fluid enters in contact with the thermocouples. The developed methodology allows tracking the flow front with accuracy in a sample stack which does not exceed 3 mm. Saturated and unsaturated permeability are compared for different fiber volume fractions, between 43 % and 64 %. The decrease of permeability with increased fiber volume fraction is coherent with the Kozeny-Carman's relation. Thanks to the high resolution in pressure measurement, transient effects can be evidenced in a single ply.*

Keywords: transverse permeability; transient effects; experimental characterization; thermocouple

1. Introduction

The transverse permeability characterization of fibrous reinforcements is of crucial importance for modelling Liquid Composite Moulding (LCM) processes, particularly when transverse flows are promoted or unavoidable such as when manufacturing thick composite parts or for infusion-driven processes. Some experimental set-ups have been proposed so far to identify the saturated permeability in transverse direction and provide reliable data – see [1] for instance. However, although it is admitted that transient permeability can largely differ from saturated permeability in the longitudinal direction [2,3], very little attention has been paid to transverse permeability, which however exhibits the same saturated/transient contrast [3]. The main difficulty raising in the characterization of transient transverse permeability is to obtain the position of the fluid front *in situ*, through small distances (thicknesses) and without disturbing the local flow. This front tracking can hardly rely on optical measurement like in planar permeability for instance [3,4]. Recently, some authors propose to use ultrasonic wave propagation to detect the flow front [5]. In this study, we propose to use micro-thermocouples to track the flow front through temperature gradient within the plies stack.

2. Experimental set-up

2.1 Transverse permeability test rig

The transverse permeability test rig is composed of a cylinder where the fluid – here, cold water – is collected and flows through the sample. A pressurized reservoir is used to inject the fluid in the cylinder and a flow control valve is added between the reservoir and the cylinder. A pressure sensor is placed in the cylinder, upstream of the sample. This sensor has a measurement range of 0-350 mbar of differential pressure and a precision of 3.5 mbar. Micro-thermocouples are placed between each ply to detect the flow front progression in the sample. Synchronous

acquisition of the signals is performed by a multimeter Hioki LR8431-20 at a sampling frequency of 100 Hz.

Figure 1.a represents a complete view of the cylinder supporting the sample. A detailed view of the positioning of the thermocouple is proposed Figure 1.b. The thermocouples are placed, at the center of the cylinder, between each ply during the pile-up of the sample stack. The thermocouple wires are then guided out of the sample through a small channel (see Figure 1.b). Figure 1.c displays a sectional view of the same cylinder for the sake of clarity.

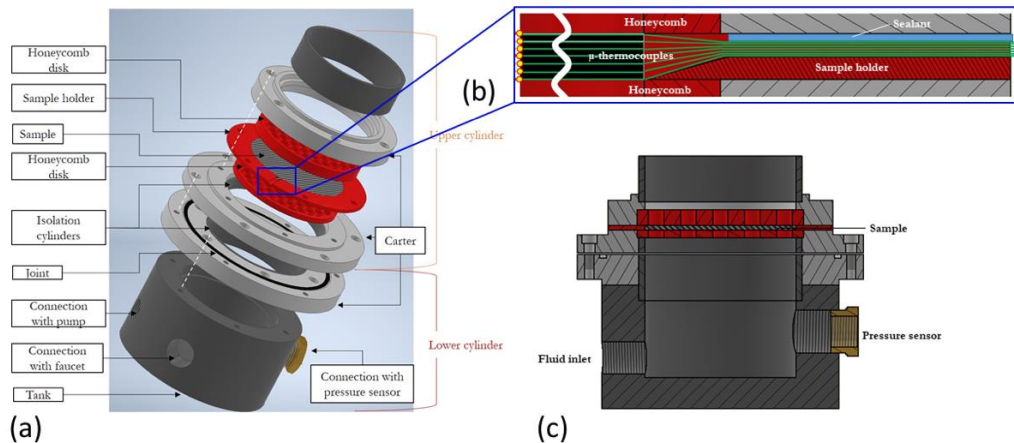


Figure 1 Transverse permeability test rig: (a) detailed view of the sample and measurement support; (b) micro-thermocouples placement within the plies and the sample support; (c) sectional view of the sample support.

2.2 Material

The tested material is a quasi-unidirectional carbon fabrics from Hexcel Corp. For this study, each ply is rotated 90° from the previous ply. The samples are cut from the fabric roll using a ring-shape cutting tool of 98 mm diameter. The tool is pressed on the fabric with a manual press and the samples are carefully cut to avoid as much as possible the separation of carbon tows from the sample edges. The fabric is impregnated with a binder which improves the resin adherence to the fibers. In order to test the material closer to industrial infusion conditions, each ply of fabric is tested only once. Three different fiber volume fractions are tested by varying the number of ply at a fixed sample height. The total sample height is 3 mm and 4 to 6 plies stacks are tested. The equivalent fiber volume fractions V_f are given in Table 1.

Note that the fiber volume fraction is calculated from the following equation [6]:

$$V_f = \frac{m}{Ah\rho} \quad (1)$$

where m is the total sample mass, A is the sample area, h the height of sample and ρ the bulk density of the fiber material. In the proposed experiments, the area of the fabric is $7.53 \times 10^3 \text{ mm}^2$ the sample height is 3 mm and the bulk density is 1800 kg/m^3 .

Table 1: Sample and experiment specifications.

ID number	1	2	3	4	5	6	7	8	9	10	11	12
Number of plies	4	4	4	4	5	5	5	5	6	6	6	6
Volume fraction V_f	0.43	0.43	0.43	0.43	0.53	0.53	0.53	0.53	0.64	0.64	0.64	0.64
v_{flu} (mm/min)	118	101	69	49	122	90	59	45	84	65	46	14

2.3 Flow front tracking

Following some work proposed by Drapier *et al.* [2] who used optical fibres to detect the fluid front advancement in stitched blanket stacks, our transverse permeability rig allows for a local detection of the flow front *in situ* by using more convenient and robust sensors, namely thermocouples. The flow front is determined from a rapid change in the local temperature measured (see Figure 2.a) – *i.e.* typically with a cold fluid in a room temperature test.

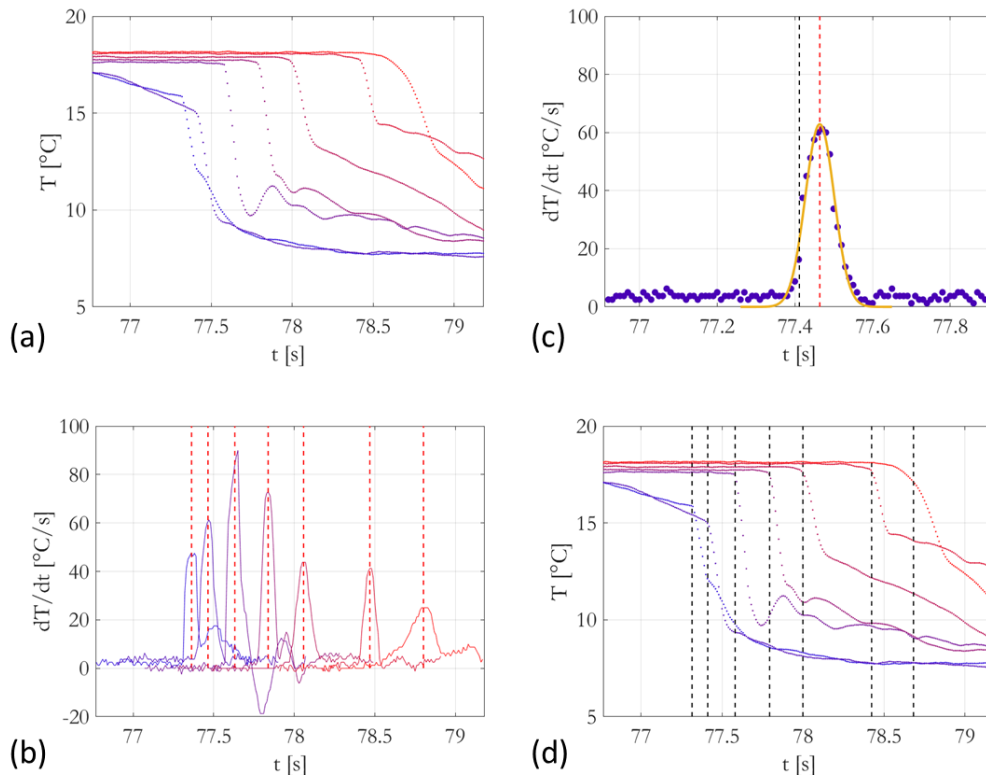


Figure 2 Flow front detection methodology based on temperature change between the air (at room temperature) and the cold water (at 7 °C): (a) thermocouples signal when the water cross the sample stack; (b) derivative of the temperature as a function of time for each thermocouple with a peak location detection, displayed with red dashed line; (c) example of fitting to obtain the peak width and determine the first point of contact between the thermocouple and water and (d) detection location of the flow front in time (sample 11).

Figure 2.b displays the temperature derivative with time. One can clearly observe the strong peaks associated with abrupt temperature decreases. To obtain more accurately the instant were the cold fluid enters in contact with the thermocouple, each peak on fig. 2.b is fitted with a Gaussian equation (see Figure 2.c) and the width of the peak is extracted. The maximum of the

derivative is not the meaningful parameter in terms of timing; instead, we use the maximum location minus the Gaussian half-width (represented as a black dashed line on fig. 2.c). Finally, the flow front advancement is represented in time-scale on fig. 2.d where black dashed lines correspond to the fluid first contact with each thermocouple.

3. Results

3.1 Pressure measurement

The pressure measurement is performed upstream of the sample and is compared with the flow front position deduced from the thermocouple signal. This allows quantifying the differential pressure needed to travel across a single ply. Figure 3 displays the pressure evolution as a function of time superimposed to the thermocouple signals. The green curve with open circles highlight the pressure delta associated with each ply. One can see that this pressure delta is not constant even if the plies are identical. Several effects could lead to such variability:

- First, the flow front may not be perfectly flat, this induces an uncertainty on the time correlation between pressure and temperature signals. The pressure signal being an average response of the fluid/sample interface while the thermocouple signal is a local measurement (typically at the center of the ply).
- The velocity of the fluid within the sample decreases with time, which also induces a pressure variation.

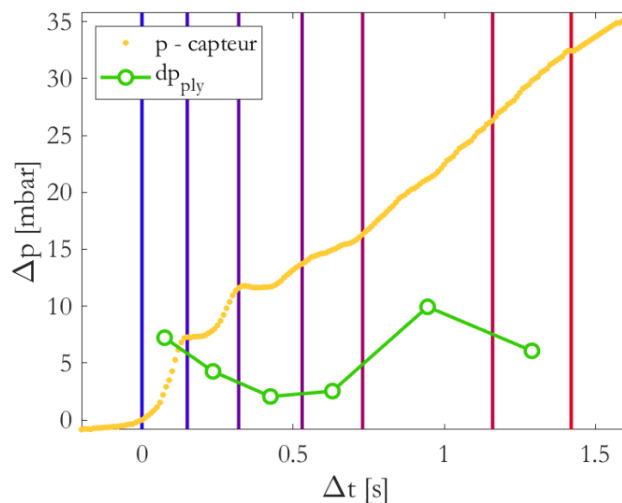


Figure 3 Pressure evolution within the sample. The yellow dots represent the pressure measured upstream minus the initial pressure at the contact of the first thermocouple. Vertical colored lines represent the thermocouple detection. The green open circles represent the delta pressure induced in each ply. (Sample 11)

3.2 Fluid velocity inside the fabric

Within the sample, three fluid velocities can be expressed. One which is related to the fluid velocity before any interaction with the sample v_{flu} , one related to the average fluid velocity during the flooding of the sample, named v_{wet} and one related to the flow front velocity in the sample named v_{dry} .

The velocity of the fluid in the cylinder, before entering in contact with the sample, v_{flu} is calculated from the pressure variation (due to the mass of the fluid column, $p = \rho g z$). This

velocity is given as a reference but might evolve when the fluid reach the sample because only the inlet pressure is kept constant. The average fluid velocity in the wet section of the sample is calculated such as:

$$v_{wet} = \frac{\Delta z_{wet,i}}{\Delta t_{wet,i}} \quad (2)$$

with $\Delta z_{wet,i}$ the cumulative sample height in the fluid – *i.e.* product of the number of saturated plies with individual ply thickness h_{ply} – and $\Delta t_{wet,i}$ the corresponding cumulative time for the number of ply i to be wetted. Finally, the flow front velocity is given by:

$$v_{dry} = \frac{h_{ply}}{\Delta t_i} \quad (3)$$

with h_{ply} , the individual ply thickness and Δt_i the corresponding time for the i^{th} ply to be saturated.

Figure 4 shows an example of the evolution of the fluid velocity as a function of the flow front advancement within the sample stack, compared with the inlet fluid velocity. The fluid velocity v_{wet} is significantly larger than the inlet fluid velocity due to the reduced (porous) efficient surface at iso-flow rate. Also, the average flow front velocity v_{wet} tends to decrease with fluid advancement due to increased pressure resistance.

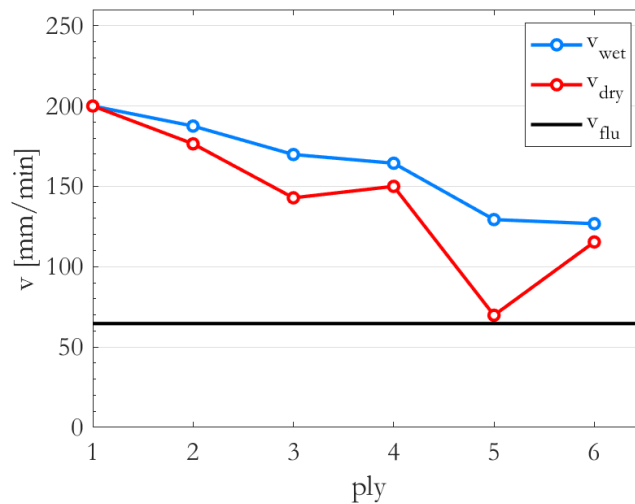


Figure 4 Fluid velocity within the sample stack as a function of the position in the sample for sample 11.

3.3 Saturated and unsaturated permeability

The saturated permeability is expressed from the 1D Darcy's law through the following expression [3, 8]:

$$k_{z\ sat} = \frac{\mu h v_{out}}{\Delta p_{tot}}, \quad (4)$$

with μ the fluid dynamic viscosity, h the sample stack thickness, v_{out} the flow front velocity downstream of the sample and Δp_{tot} the pressure gradient, both in steady state flow. The flow front velocity v_{out} is calculated, once steady state is reached, from a linear fit of the pressure evolution (since the pressure variation is only due to the mass of the fluid column after the sample is saturated). The total pressure gradient Δp_{tot} is calculated by differentiating the

pressure at steady state flow to the pressure once the flow is interrupted. Finally, the viscosity of water is adjusted for each experiment considering the temperature of the fluid at steady state flow. Results of the saturated permeability are displayed in Figure 5.b as a function of fiber volume fraction.

The unsaturated permeability is expressed as follow [3, 8]:

$$k_{z \text{ unsat}} = \frac{(1-V_f)\mu z(t)^2}{2\Delta p(t)t}, \quad (5)$$

with z the fluid position in the sample, Δp the pressure gradient in the sample and t the time for the fluid to saturate the considered sample thickness z . In order to obtain quantitative estimation of the unsaturated permeability, we propose to fit Equ. 5 to the flow front position obtained by the thermocouples – i.e. square of flow front position vs. time multiplied by pressure gradient. A linear fit is performed without taking into account the last thermocouple signal since the positioning error in the z -direction is not perfectly known (the thermocouple might be slightly above the ply free surface) (see Figure 5.a). The results are displayed on Figure 5.b as a function of fiber volume fraction. The error bar represents the standard deviation calculated on four experiments.

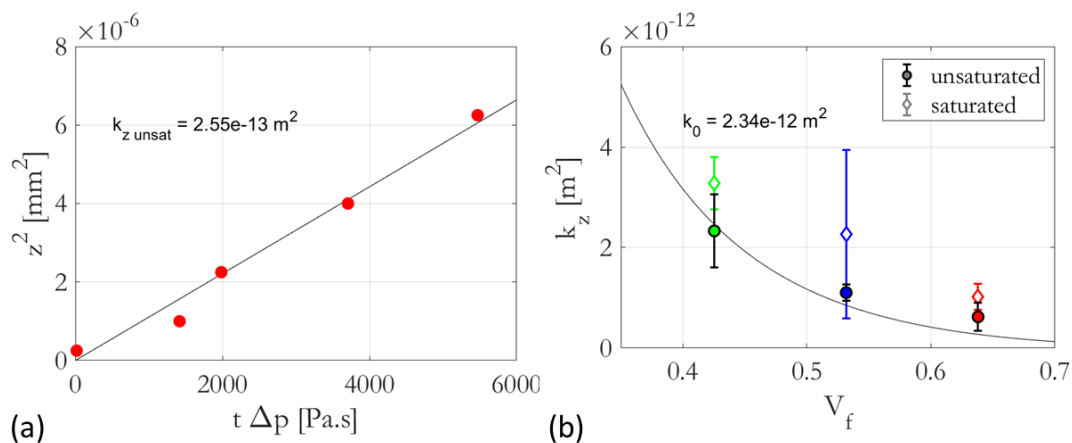


Figure 5 Unsaturated permeability calculation: (a) fit of Equ. 4 on the set of data (sample 12) without taking the last thermocouple signal (each data point correspond to a thermocouple detection signal) ; (b) Average unsaturated permeability as a function of fiber volume fraction. The error bar represents the standard deviation calculated on 4 experiments. The black line represents Eq. 6 best fit to the data.

The analytical Kozeny-Carman's equation, which relates the permeability to the volume fraction, is given in [7]:

$$k_z = k_0 \frac{(1-V_f)^3}{V_f^2}, \quad (6)$$

with k_0 a coefficient of permeability. The fitted coefficient to the unsaturated permeability is equal to $2.34 \times 10^{-12} \text{ m}^2$ and the obtained curve is plotted as a black line in Figure 5.b.

4. Discussion

The ratio $k_r = \frac{k_{z \text{ unsat}}}{k_{z \text{ sat}}}$ is equal to 0.61, 0.49 and 0.71 for V_f equal to 0.64, 0.53 and 0.43, respectively. This is in good agreement with the range reported by Park and Krawczak [3] who relate the ratio k_r to the degree of saturation (presence of air bubbles during the unsaturated

flow). This assumption leads to the conclusion that unsaturated permeability is smaller than saturated permeability, as seen in our experiments [3].

In addition to classical permeability measurements, an interesting pressure evolution for each ply is evidenced as shown in Figure 6, for two distinct fluid inlet velocities. Statistically, the position of the inter-ply detected by the thermocouples is located at the end of the steep increase in pressure and just before the plateau. This would imply that the transient pressure within one ply is first composed of a low pressure increase (or decrease) followed by a steep increase until it reaches the top of the ply. At this stage of our work, it is not possible to decipher the cause of this complex variation. It could be due to the fiber fraction volume difference between the inter-ply (lower fraction) and in the ply (higher fraction). Further investigations are needed to elucidate these observations. However, this phenomenon seems to persist at fluid velocity from 14 to 120 mm/min and independently of the fiber volume fraction, within the range tested.

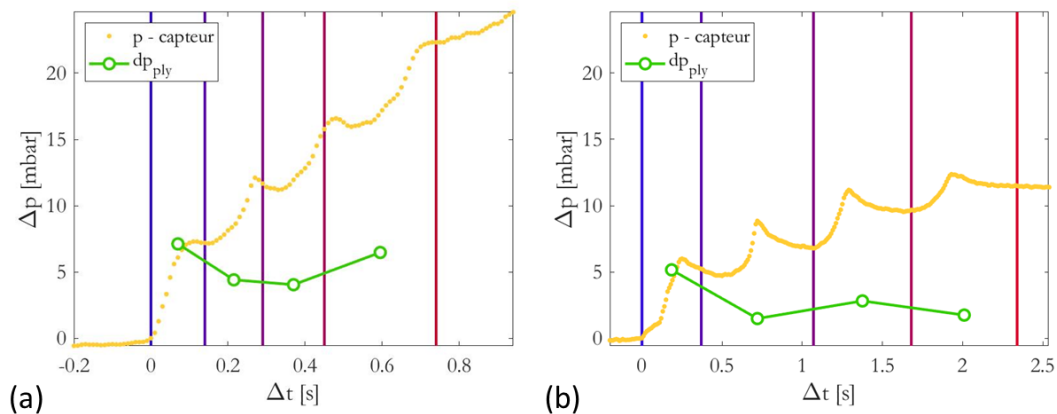


Figure 6 Pressure evolution as a function of time within the sample: (a) test on 4 plies stack sample with a fluid inlet velocity of 118 mm/min (Sample 1) and (b) 69 mm/min (Sample 3).

5. Conclusions

We developed a new transverse permeability test rig for the measurement of saturated and unsaturated regimes based on thermocouple detection of the fluid flow front. The use of water as test fluid allows a great experimental ease and improves the repeatability of the test by reducing cleaning complications. The main results obtained from this study are:

- Permeability measurements are consistent with the Kozeny-Carman's equation on the range of fiber volume fraction tested.
- The ratio of unsaturated to saturated permeability k_r is around 0.6 - 0.7, for this carbon UD fabric infused with water.
- Some very particular pressure evolution can be evidenced in each ply. Which are still under investigation at this stage.

The sensibility of the sensors allows following small-scale variations in the pressure profile and correlating them to statistically probable location within the stack. This work is preliminary and more experiments will certainly bring some new insights in the understanding of transient permeability.

Acknowledgements

The authors acknowledge the technical support provided by Eric Garrigou to the development of this test bench.

6. References

1. R. Nunez, Problématique de la mesure de la perméabilité transverse de préformes fibreuses pour la fabrication de structures composites. PhD thesis Mines Saint-Etienne, 2009.
2. S. Drapier, J. Monatte, O. Elbouazzaoui, and P. Henrat, Characterization of transient through-thickness permeabilities of Non Crimp New Concept (NC2) multiaxial fabrics, *Composites Part A*: 36(7) 877-892, 2005.
3. C.H.Park and P. Krawczak, Unsaturated and saturated permeabilities of fiber reinforcement: Critics and suggestions, *Front. Mater.* 2:38, 2015.
4. R. Arbter, et al., Experimental determination of the permeability of textiles: A benchmark exercise, *Composites Part A*, 42 (9) 1157-1168, 2011.
5. F. Lionetto, F. Montagne and A. Maffezzoli, Out-of-plane permeability evaluation of carbon fiber preforms by ultrasonic wave propagation, *Materials*. 13:2684, 2020.
6. A. Yong, et al., Out-of-plane permeability measurement for reinforcement textiles: A benchmark exercise, *Composites Part A: Applied Science and Manufacturing* 148 106480, 2021.
7. P.C. Carman, Fluid flow through granular beds. *T I Chem Eng-Lond*, 15:150–6, 1937.
8. D. Salvatori, B. Caglar, H. Teixido and V. Michaud, Permeability and capillary effects in a channel-wise non-crimp fabric, *Composites Part A*: 108 41:52, 2018.